

IFSCC 2025 full paper (IFSCC2025-770)

## The ferment of an endophytic fungi *Umbelopsis dimorpha*: a superior substitute for *Tricholoma matsutake*

Lu Hu \*<sup>1,2</sup>, Kun Dai <sup>3</sup>, Huixian Xu <sup>1</sup>, Jiaheng Zhang <sup>2</sup>, Song Jiao <sup>3</sup>, Chujie Huang <sup>\*1</sup>

<sup>1</sup> R&D Department, SHE LOG (Guangzhou) Biotechnology Co., Ltd, Guangzhou;

<sup>2</sup> Sauvage Laboratory for Smart Materials, Harbin Institute of Technology, Shenzhen;

<sup>3</sup> Hangzhou Jajale Biotech Co., Ltd, Hangzhou, China.

### 1. Introduction

*Tricholoma matsutake* is a type of mycorrhizal fungus, recognized as a rare and valuable natural therapeutic fungus globally, which has been utilized as food and in traditional Chinese medicine for millennia in East Asian nations <sup>[1]</sup>. *T. matsutake* is rich in protein, amino acids, sterols, polypeptides, and other rare elements <sup>[2]</sup>. *T. matsutake* has been documented to exhibit several physiological effects, including anti-cancer, anti-inflammatory, hepatoprotection, and antimicrobial properties <sup>[3,4]</sup>. Moreover, *T. matsutake* possesses whitening, anti-photoaging, skin repair, and anti-wrinkle properties, among other skincare advantages <sup>[5,6]</sup>. Prior research has demonstrated that mycelial preparations of *T. matsutake* exhibit inhibitory effects on tyrosinase, hence diminishing melanin synthesis <sup>[7]</sup>, as well as inhibiting MMP-1 <sup>[6]</sup>, promoting the proliferation of HaCaT cells, and facilitating wound healing in murine models <sup>[1]</sup>. Nonetheless, because of the challenges associated with artificial culture, the propagation of matsutake has consistently depended on natural forest growth, alongside the diminished extraction efficiency of conventional extraction methods, etc., hence enhancing the value of *T. matsutake* and the development costs of *T. matsutake*-related products.

It is important to note that endophytic fungi, which dwell in fungal fruiting bodies in a symbiotic relationship <sup>[8]</sup>, have no evident damage to host cells, are a rich source of novel bioactive compounds, and are intimately tied to the formation and proliferation of fungal fruiting bodies <sup>[9]</sup>. Endophytic fungi can not only produce metabolites with medicinal value similar to those of host plants but also directly produce secondary metabolites with biological activity to enhance the adaptability of host plants <sup>[1,9]</sup>. In recent years, metabolites isolated from endophytic fungi usually include polyketides, terpenoids, and steroids <sup>[10]</sup>. These metabolites have various pharmacological activities, such as anticancer, antioxidant, and antibacterial <sup>[11]</sup>. However, the endophytic fungi of *T. matsutake* have not been studied, and their various benefits have never been explored.

This study isolated an endophytic fungus, *Umbelopsis dimorpha*, from the fruiting bodies of *T. matsutake* and used it for fermentation to obtain fungal extract (UFE). To compare the UFE with *T. matsutake* extract (TME), the skincare activity and safety of UFE and TME were evaluated, including the anti-tyrosinase activity, MMP-1 inhibition, cell repair capability, and cytotoxicity of human dermal fibroblasts. Then, non-target metabolomics analysis of UFE and

TME was performed based on UPLC-Q-TOF-MS/MS, and the different metabolites between them were analyzed by principal component analysis (PCA) and orthogonal partial least squares discriminant analysis (OPLS-DA). This study provides valuable information on endophytic fungi and their metabolites in *T. matsutake* fruiting bodies and expands their application.

## 2. Materials and Methods

### 2.1. Materials and chemicals

Fresh *matsutake* fruiting bodies were obtained from a cultivation field in Shangri-La, Yunnan Province, China. After harvest, fruiting bodies of similar size and shape without any physical damage were selected, immediately stored in microbial-free sacks, and transferred to the laboratory for subsequent analysis. All other chemicals and organic solvents were analytical grade and available from the regular reagent platform.

### 2.2. Isolation and preparation of fungal extract

The techniques for isolating and identifying endophytic fungi are based on prior research [9] with certain modifications. The strain was cultivated in potato dextrose broth (PDB) and incubated at 30°C for 5 days to create fungal extracts. Then, the supernatant was freeze-dried and stored at -20°C for further analysis. The blank control was a bacteria-free PDB medium; all other techniques were identical.

A second extraction were performed on PDB medium, *Umbelopsis* fermentation samples, and *T. matsutake* by Ultrasonic extraction with 50% ethanol for 30 minutes. The blank control extract (BCE), *Umbelopsis* fermentation extract (UFE), and *T. matsutake* extract (TME) were freeze-dried from filtrates<sup>[1]</sup>.

### 2.3 Anti-tyrosinase activity

BCE, UFE, and TME were dissolved in DMSO and diluted to 800 µg/ml with 0.05 M phosphate buffer (ph 6.8). Mix 60 µL sample with 30 µL tyrosinase solution (100 U/mL in phosphate buffer) and incubate at 37°C for 10 minutes. Next, add 120 µL of L-dopa (1 mg/ml) and incubate at room temperature for 5 minutes. The sample blank was made using 30 µL buffer instead of tyrosinase solution. Control samples included DMSO instead of the test ingredient. The enzyme solution was replaced with 30 µL of buffer in the control blank. Multiskan GO 1510 (Thermo Fisher Scientific, Vantaa, Finland) detected absorbance at 475 nm. The experiment was tripled, and the relative cell viability was calculated.

### 2.4 MTT cytotoxicity

100 µL of the human fibroblast solution was dispensed into a 96-well plate and incubated for 24 hours. The cultured cells were exposed to different doses of UFE and TME for 24 hours, after which 10 µL of MTT solution was added for 4 hours of incubation. The growth media was removed, and 150 µL of DMSO was added to the cultured cells. The absorbance at 490 nm was measured, and the relative cell viability was calculated.

### 2.6. Matrix metaloproteinase-1 (MMP-1) activity

Twenty-four hours post-seeding, the human fibroblast suspensions were subjected to varying doses of UFE and TME and incubated for 48 hours. TGF-β1 was the positive control, while PBS buffer was the blank control. The cell supernatant was obtained for MMP-1 analysis with the MMP-1 ELISA kit (Multisciences Biotech, Co., Ltd.).

### 2.7. Cell scratch assay

The cell scratch assay was performed according to the reported protocol as described [12]. The human fibroblast suspensions were cultured for 18 to 24 hours, and the wounds were created using a plastic tip. The cells were subsequently cultured for 24 hours in the growth media (blank control) or subjected to varying doses of UFE and TME. The wound distance was assessed using IPP image analysis software, measuring the scratch width of both treated and untreated groups.

### 2.8. UPLC-Q-TOF-MS/MS analysis

UFE, TME, and BCE were dissolved in 70% methanol and centrifuged (12000 rpm, 4°C, 15 min) to extract supernatants for UPLC-Q-TOF-MS/MS analysis. The analytical sample was prepared by combining 25 µL of each sample. The Waters Vion-IMS system was used to analyze samples with Acquity UPLC I-Class Plus and ACQUITY UPLC BEH C18 column (1.7 µm, 2.1 mm\*100 mm). Data was collected using UNIFI (v1.9).

The raw data was deconvolved using Waters Progenesis QI (v 3.0.3.0). QC files were selected as a reference for peak extraction, alignment, and area normalization. The compounds were qualitatively compared by Metlin 2019, NIST, YMDB (<https://www.ymdb.ca/>), PAMDB (<http://pseudomonas.umaryland.edu/>), and ECMDB (<https://ecmdb.ca/>).

### 2.9. Statistical analysis

PCA and OPLS-DA analysis were performed using MetaboAnalyst 5.0 (<https://www.metaboanalyst.ca/>). Heatmap visualization was done with R (<http://www.R-project.org>). Data is presented as mean ± standard deviation (SD). ANOVA was used to compare treatments and samples.

## 3. Results and Discussion

### 3.1. Identification of endophytic fungus

The isolate's chromosomal DNA was extracted, and the ITS region was amplified using polymerase chain reaction (PCR) and subsequently sequenced. Phylogenetic analysis of the ITS region revealed a complete match with the sequence of *Umbelopsis* sp. Isolate Cg01. The macroscopic assessment of the isolate indicated that the fungus exhibited a filamentous structure with a velvety white mycelium on the colony surface (Figure 1), aligning with the morphological characterization of *Umbelopsis* as documented [22]. Consequently, this endophytic fungus is designated as *Umbelopsis* sp. TM01.



**Figure 1.** Morphological characteristics of *Umbelopsis* sp. TM01. Front (a) and back (b) of *Umbelopsis* sp. TM01 was grown on PDA medium.

### 3.2. In vitro whitening efficacy evaluation

Tyrosinase is a crucial enzyme in pigment formation, and its inhibition is a prevalent method for diminishing pigment spots; thus, tyrosinase inhibitors are often utilized as whitening treatments in cosmetics [13]. The anti-tyrosinase activities of BCE, UFE, and TME were assessed. The results revealed that the tyrosinase inhibitory activity of UFE was approximately four times more than that of TME, indicating a more potent inhibitory effect on tyrosinase (Figure 2).

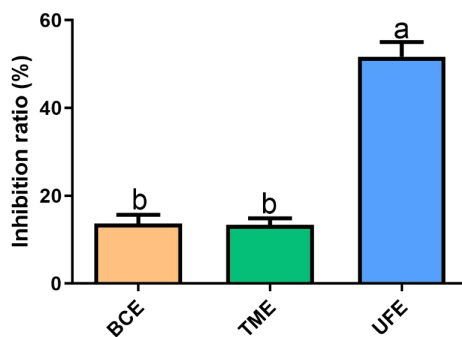


**Figure 2.** Inhibitory action of tyrosinase by BCE, UFE, and TME. The distinct superscript letters exhibit a statistically significant difference at  $p < 0.05$ .

### 3.3. Safety assessment by MTT cytotoxicity

Testing the toxic effects of various materials on cells enables the rapid identification of samples with potential cytotoxicity. Its cytotoxicity was assessed to determine the optimal UFE concentration for treating human skin fibroblasts to determine its anti-wrinkle and cellular healing effects. Succinate dehydrogenase in mitochondrial cells converts exogenous MTT into insoluble blue-purple crystalline formazan stored in cells. Necrotic cells lack this activity. MTT can measure cell survival. Figure 3 shows that BCE and TME had CV90s of 2.85% and 1.91%, respectively, for cytotoxicity. At 10% concentration, UFE's cell survival rate exceeded 90%, showing that it is non-toxic to human dermal fibroblasts and safer than the two control groups, paving the way for its greater use in cosmetics.

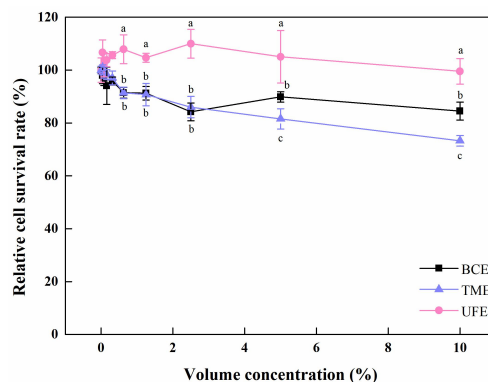


**Figure 3.** Relative survival rate of human dermal fibroblasts under different treatments. The distinct superscript letters exhibit a statistically significant difference at  $p < 0.05$ .

### 3.4 Cellular anti-wrinkle efficacy evaluation

The emergence of wrinkles is a principal attribute of skin aging. The primary cause of wrinkle development is the depletion of collagen in the dermal layer of the skin. Ultraviolet factors can stimulate MMP-1 expression and hinder collagen production. MMP-1, a member of the matrix metalloproteinase family, degrades various collagen and extracellular matrix components, hence playing a crucial role in developing skin wrinkles. Thus, the anti-wrinkle

effectiveness of the samples can be evaluated by measuring the reduction of MMP-1 activity. Previous research [6] demonstrated that *T. matsutake* mycelia extract dose-dependently inhibited elastase activity and MMP-1 levels. Identifying compounds that suppress MMP-1 expression may suggest their anti-wrinkle properties. BCE, UFE, and TME were tested for anti-wrinkle effects by reducing MMP-1 expression. Figure 4 shows that TME did not significantly mitigate MMP-1 expression at test dosages, whereas UFE did. At concentrations of 0.3125% of UFE, MMP-1 expression levels were lowered by  $18.90 \pm 4.09\%$ , indicating greater inhibitory effects than TME and a strong anti-wrinkle effect.

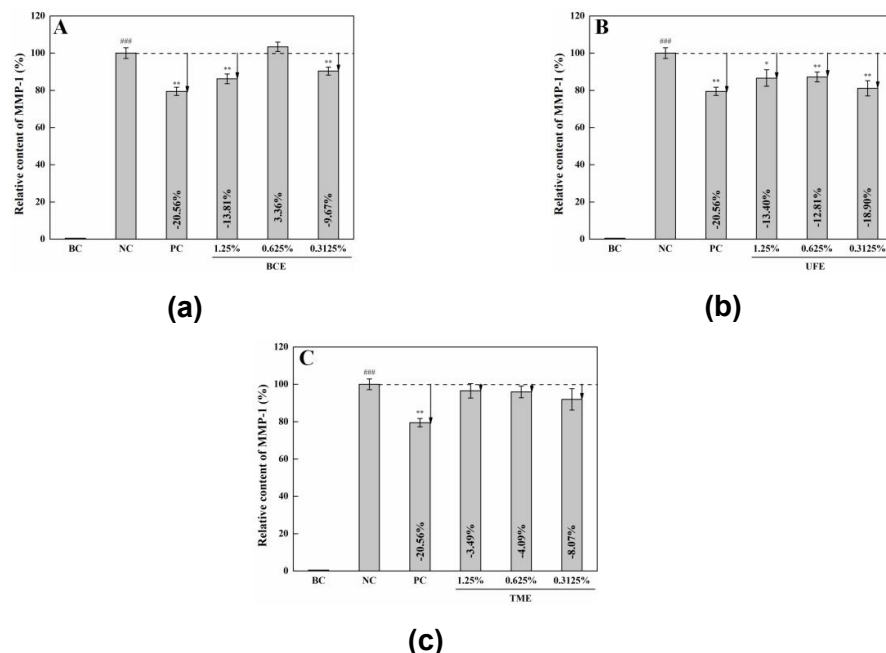


**Figure 4.** Effects of BCE (a), UFE (b), and TME (c) on the level of MMP-1 in human dermal fibroblasts. The t-test was used for analysis. Compared with the BC group (blank control),  $p < 0.001$  was indicated as \*\*\*. Compared with the NC group (negative control),  $p < 0.05$  was indicated as \*, and  $p < 0.01$  was indicated as \*\*.

### 3.5. Cellular repair effect evaluation

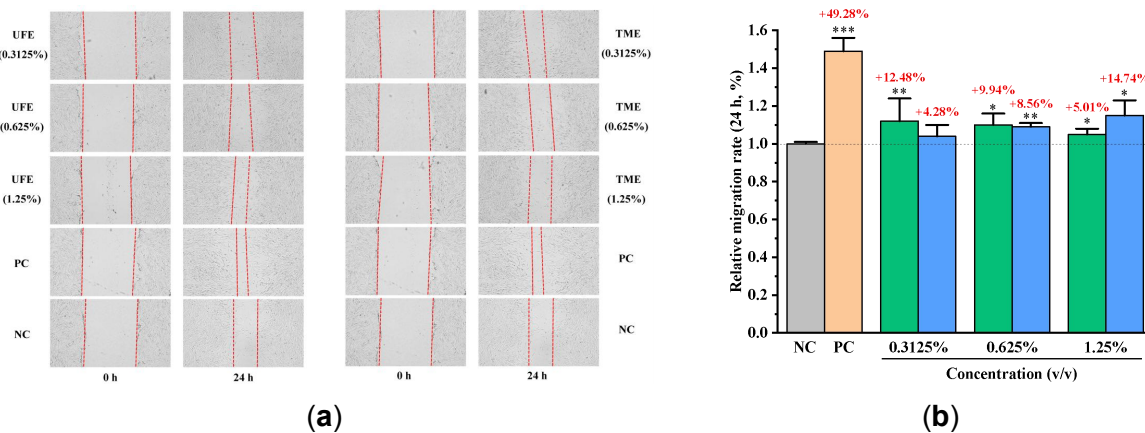


**Figure 5.** Cellular repair effect of different groups (UFE and TME). (a) Cell migration images; (b) Relative migration rates. The t-test was used for analysis. Compared with the NC group (negative control),  $p < 0.05$  was indicated as \*,  $p < 0.01$  was indicated as \*\*, and  $p < 0.001$  was indicated as \*\*\*.

The cell scratch assay is an expedited technique for assessing cell migration and motility, utilized to evaluate cellular repair capabilities. Zhu et al. (2021) [1] discovered that the extract

from the mycelia of *T. matsutake* enhances the proliferation of HaCat cells and facilitates wound healing in mice using animal models. Given the above, an *in vitro* wound healing model was established to investigate the effects of UFE and TME on cellular migration and repair, prompted by cell migration during the healing process. The findings indicated that the relative migration rate of UFE markedly escalated at concentrations of 1.25%, yielding repair rates of 14.74% (Figure 5). Moreover, a comparison of the wound-healing efficacy between the UFE group and the TME group revealed no significant differences across all tested concentrations, suggesting that the wound-healing effect of UFE is analogous to that of TME.

### 3.6. PCA analysis of BCE, UFE, and TME

The data show that UFE has better anti-tyrosinase and anti-wrinkle effects than TME. UFE recovers cells like TME. UFE was non-toxic to human dermal fibroblasts at all concentrations below 10%, while TME has a CV90 of 1.91%. Because UFE is more effective than TME, a non-targeted metabolomics technique based on UPLC-Q-TOF-MS/MS was used to compare their activities. The BCE, UFE, and TME groups had 8226, 9390, and 8992 metabolite ion signatures, identifying 2137 metabolites via the metabolome database. PCA is an unsupervised method to identify essential differences between samples and measure aggregation and dispersion. Based on quantitative metabolite data, the metabolic profiles demonstrated significant differences between the UFE, TME, and BCE groups. Figure 6 shows that the first PC (PC1) and second PC (PC2) accounted for 62.4% and 22% of the variance, respectively. The UFE group had significantly different metabolic profiles from the TME and BCE groups, showing that their metabolic profiles are distinct. This may indicate changes in physiological status, function, or therapeutic responses, helping to clarify metabolic disparities across groups.

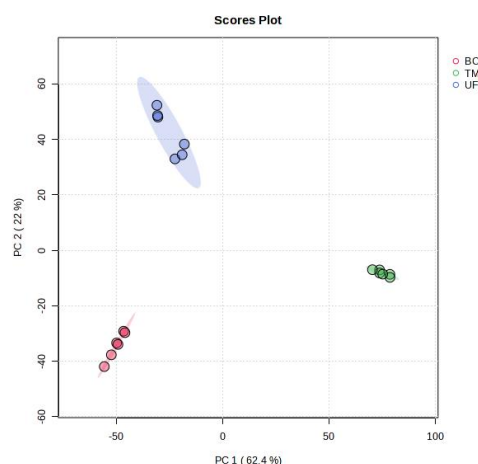


**Figure 6.** PCA plot of BCE, UFE, and TME.

### 3.7 Screening and analysis of differential metabolites

OPLS-DA was then used to compare UFE and TME actives. The OPLS-DA score map (Figure 7a) showed significant metabolite differences between UFE and TME groups. For OPLS-DA model evaluation, cross-validation with a 10-fold CV algorithm was used. One hundred permutation tests of the OPLS-DA model (Figure 7b) showed that it was fitting well and had reliable predictability, so it could be used to screen differential metabolites [24]. Out of 375 differential metabolites identified through screening, 232 were up-regulated and 143 were down-regulated in the UFE group compared to the TME group (Figure 7c).

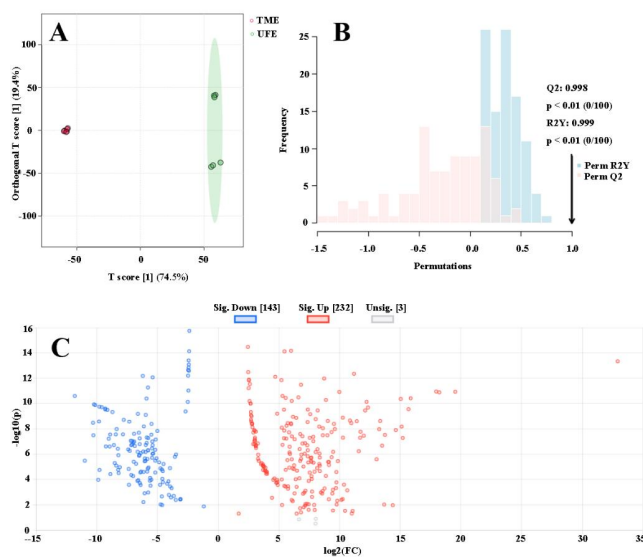


**Figure 7.** Metabolites differ between the UFE and TME groups. (A) OPLS-DA score plots for UFE and TME groups; (B) 100-permutation test of the model; (C) volcano map of differential metabolites. The volcano graphic shows blue dots for down-regulated metabolites, red dots for up-regulated differential metabolites, and grey dots for discovered but not substantially different metabolites.

### 3.8 Classification of the differential metabolites

To explain the differences between groups, metabolites were divided into six super-classes: carbohydrates and carbohydrates, organic acids and derivatives, lipids and lipid-like molecules, alkaloids and derivatives, benzenoids, phenylpropanoids, and polyketides (Figure 8). Most TME metabolites were found in UFE, but in different amounts. Our findings are supported by other research showing that endophytic fungal microbiomes from plants can synthesize secondary metabolites like alkaloids, terpenoids, flavonoids, and phenols [14]. As shown in Figure 8, UFE produced significantly more alkaloids and derivatives, benzenoids, phenylpropanoids, and polyketides than TME and BCE, indicating that UFE ferments both medicinal and unique secondary metabolites. Secondary metabolites may boost UFE's anti-tyrosinase, anti-wrinkle, and regenerative properties. Thus, we study the secondary metabolite UFE and TME chemical compositions.

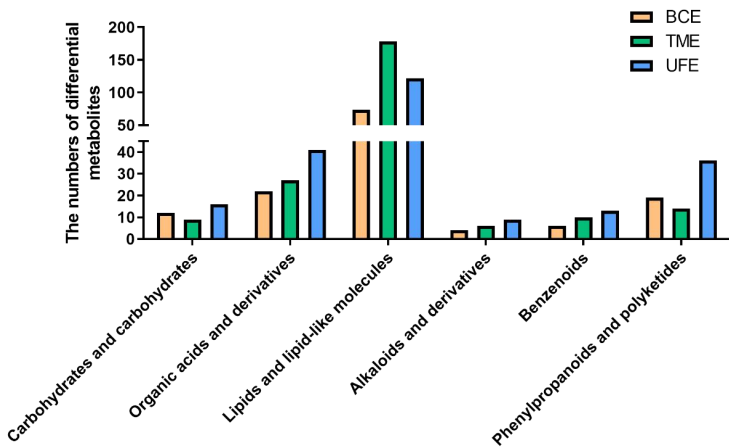


**Figure 8.** The number of differential metabolites in BCE, UFE, and TME groups at the chemical superclasses.

### 3.9 Analysis of metabolic characteristics of differential metabolites

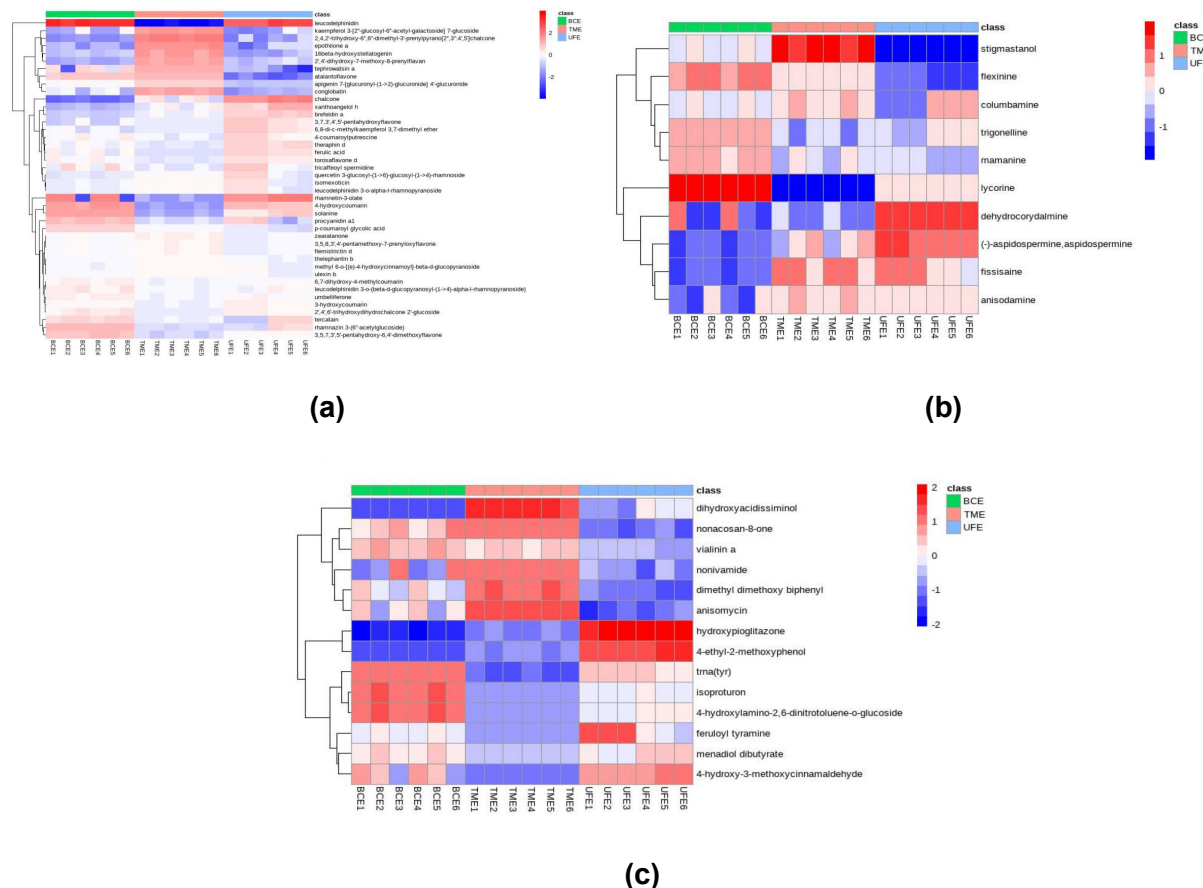


**Figure 9.** Heatmap analysis of Phenylpropanoids and polyketides compounds (a), Alkaloids and derivatives (b), and Benzenoids (c) in the BCE, UFE, and TME groups.

A heatmap showed the diverse metabolites of the three chemical super-classes: phenylpropanoids and polyketides, alkaloids and derivatives, and benzenoids (Figure 9). Fungal secondary metabolites, phenylpropanoids and polyketides, are most prevalent and well-characterised [15]. Two metabolic pathways—phenylalanine, which creates polyketones, and mehydroxy acid and the 1-DOXP path, which produces isopentenes—converge to make these molecules. Only Rutaceae, Apiaceae, Compositae, Legumes, and other plant families have oxypentenylation secondary metabolites at very low levels. [16]. Chalcone, xanthoangelol h, brefeldin a, 3,7,3',4',5'-pentahydroxyflavone, 6,8-di-c-methylkaempferol 3,7-dimethyl ether, 4-coumaroylputrescine, ferulic acid, and torosaflavone d were enriched in UFE compared to TME and BCE (Figure 9a). Dehydrocorydalmine and (-)-aspidospermine were enriched in UFE compared with TME and BCE (Figure 9b). Hydroxypioglitazone and 4-ethyl-2-methoxyphenol, belonging to the subclass of benzenoids, were enriched in UFE compared with TME and BCE (Figure 9c).

Chalcones and their derivatives block tyrosinase and activate the glycolytic pathway for improved anti-aging benefits [17]. 3,7,3',4',5'-pentahydroxyflavone, possesses good antioxidant and anti-tyrosinase activity [18]. 6,8-di-c-methylkaempferol 3,7-dimethyl ether is a kaempferol derivative. Kaempferol can dock to the active center of tyrosinase and prevent substrate binding by occupying the active site, thus reducing the catalytic activity of tyrosinase [19]. Keun Ha, et al. [20] found that kaempferol derivatives can inhibit the production of MMP-1 and promote cell proliferation in a dose-dependent manner in HaCaT cell

proliferation experiments. Studies have shown ferulic acid has more vigorous tyrosinase-inhibiting activity than other cinnamic acid derivatives [21]. Ferulic acid has antioxidant properties in the dermis and inhibits collagenase and elastase, improving skin penetration and reducing skin aging, according to Yücel et al. (2023) [22]. Tyrosinase and MMP-1 inhibition are also seen in 4-coumaroylputrescine [23]. In conclusion, phenylpropanoids and polyketides can inhibit tyrosinase and reduce wrinkles, making them useful skincare and anti-aging substances.

#### 4. Conclusion

Endophytic fungi are a group of host-associated fungal communities that live within the tissues of plants and form symbiotic relationships with their host plants. They frequently enhance the plant's growth, health, and stress resilience by synthesizing diverse bioactive chemicals. This research emphasizes the promise of endophytic fungi derived from *Tricholoma matsutake*, particularly the *Umbelopsis* sp. strain. TM01 is a promising source of anti-tyrosinase, anti-wrinkle, and cellular repair chemicals. The fermentation broth extract of *Umbelopsis* sp. TM01 (UFE) exhibited significant anti-tyrosinase activity, anti-wrinkle effectiveness, and cellular recovery capability. UFE is non-cytotoxic to human dermal fibroblasts at concentrations up to 10%. The metabolites found in UFE primarily consist of organic acids and their derivatives, lipids and lipid-like substances, alkaloids and their derivatives, benzenoids, phenylpropanoids, and polyketides. Among them, the secondary metabolites, including alkaloids and their derivatives, benzenoids, phenylpropanoids, and polyketides, were prevalent in UFE and are likely responsible for its activity. The above research indicated that UFE outperforms TME in skin care, which might be a cost-effective and higher-activity alternative for TME. This discovery provides a theoretical basis for studying the pharmacological activity of *T. matsutake* endophyte, lowers its application cost, and has significant ecological and economic value.

#### 5. References

- [1] ZHU W, CHEN Y, QU K, et al. Effects of Tricholoma matsutake (Agaricomycetes) Extracts on Promoting Proliferation of HaCaT Cells and Accelerating Mice Wound Healing[J]. International Journal of Medicinal Mushrooms, 2021, 23(9): 45-53.
- [2] LIU G, WANG H, ZHOU B, et al. Compositional analysis and nutritional studies of Tricholoma matsutake collected from Southwest China[J]. JOURNAL OF MEDICINAL PLANTS RESEARCH, 2010, 4(12): 1222-1227.
- [3] TAKAKURA Y. Tricholoma matsutake fruit bodies secrete hydrogen peroxide as a potent inhibitor of fungal growth[J]. Canadian Journal of Microbiology, 2015, 61(6): 447-450.
- [4] KAPLANER E, AYDOĞMUŞ-ÖZTÜRK F, ÖZTÜRK M, et al. Anatoluin A and B isolated from medicinal Tricholoma anatomicum are new cytotoxic ergostanoids against the most common cancers[J]. Natural Product Research, 2023, 37(22): 3787-3797.
- [5] YANG S, QUAN Q, LI X, et al. Evaluation of Whitening Effect of Tricholoma matsutake Extract Ointment on Guinea Pig Model of Chloasma[J]. LATIN AMERICAN JOURNAL OF PHARMACY, 2023, 42(4): 924-933.
- [6] KIM S Y, GO K C, SONG Y S, et al. Extract of the mycelium of *T. matsutake* inhibits elastase activity and TPA-induced MMP-1 expression in human fibroblasts[J]. International Journal of Molecular Medicine, 2014, 34(6): 1613-1621.
- [7] 최상윤, 김나나, 김영언, et al. Inhibitory Effects of Cultured Tricholoma matsutake Mycelia on Melanin Biosynthesis[J]. 한국식품과학회지, 2011, 43(2): 240-242.

- [8] TAN W N, NAGARAJAN K, LIM V, et al. Metabolomics Analysis and Antioxidant Potential of Endophytic Diaporthe fraxini ED2 Grown in Different Culture Media[J]. *Journal of Fungi* (Basel, Switzerland), 2022, 8(5): 519.
- [9] MA Y, GAO W, ZHANG F, et al. Community composition and trophic mode diversity of fungi associated with fruiting body of medicinal Sanghuangporus vaninii[J]. *BMC microbiology*, 2022, 22(1): 251.
- [10] ZHENG R, LI S, ZHANG X, et al. Biological Activities of Some New Secondary Metabolites Isolated from Endophytic Fungi: A Review Study[J]. *International Journal of Molecular Sciences*, 2021, 22(2): 959.
- [11] NAGARAJAN K, IBRAHIM B, AHMAD BAWADIKJI A, et al. Recent Developments in Metabolomics Studies of Endophytic Fungi[J]. *Journal of Fungi* (Basel, Switzerland), 2021, 8(1): 28.
- [12] LIANG C C, PARK A Y, GUAN J L. In vitro scratch assay: a convenient and inexpensive method for analysis of cell migration in vitro[J]. *Nature Protocols*, 2007, 2(2): 329-333.
- [13] MINSAT L, PEYROT C, BRUNISSEN F, et al. Synthesis of Biobased Phloretin Analogues: An Access to Antioxidant and Anti-Tyrosinase Compounds for Cosmetic Applications[J]. *Antioxidants* (Basel, Switzerland), 2021, 10(4): 512.
- [14] XINGYUAN Z, LINJUN M, FANG C. The medicinal potential of bioactive metabolites from endophytic fungi in plants[J]. *eFood*, 2022, 3(4): e28.
- [15] ALAM B, LÍ J, GĚ Q, et al. Endophytic Fungi: From Symbiosis to Secondary Metabolite Communications or Vice Versa?[J]. *Frontiers in Plant Science*, 2021, 12: 791033.
- [16] FIORITO S, EPIFANO F, PREZIOSO F, et al. Biomolecular Targets of Oxyperenylated Phenylpropanoids and Polyketides[J]. *Progress in the Chemistry of Organic Natural Products*, 2019, 108: 143-205.
- [17] WU Y, WANG H, ZHU J, et al. Licochalcone A activation of glycolysis pathway has an anti-aging effect on human adipose stem cells[J]. *Aging*, 2021, 13(23): 25180-25194.
- [18] SARI R K, PRAYOGO Y H, SARI R A L, et al. Intsia bijuga Heartwood Extract and Its Phytosome as Tyrosinase Inhibitor, Antioxidant, and Sun Protector[J]. *FORESTS*, 2021, 12(12): 1792.
- [19] LI X, GUO J, LIAN J, et al. Molecular Simulation Study on the Interaction between Tyrosinase and Flavonoids from Sea Buckthorn[J]. *ACS omega*, 2021, 6(33): 21579-21585.
- [20] LEE K H, 공혜진, CHO Y L, et al. Anti-Microbial and Anti-Wrinkle Effect of Kaempferol and Kaempferol Rhamnosides isolated from Hibiscus cannabinus L.[J]. *한국약용작물학회지*, 2012, 20(6): 454-460.
- [21] LEE H S. Tyrosinase inhibitors of Pulsatilla cernua root-derived materials[J]. *Journal of Agricultural and Food Chemistry*, 2002, 50(6): 1400-1403.
- [22] YUCEL C, KARATOPRAK G S, ILBASMIS-TAMER S, et al. Ferulic acid-loaded aspasomes: A new approach to enhance the skin permeation, anti-aging and antioxidant effects[J]. *JOURNAL OF DRUG DELIVERY SCIENCE AND TECHNOLOGY*, 2023, 86: 104748.
- [23] KIM S B, LIU Q, AHN J H, et al. Polyamine derivatives from the bee pollen of Quercus mongolica with tyrosinase inhibitory activity[J]. *BIOORGANIC CHEMISTRY*, 2018, 81: 127-133.